Fungal LysM effectors that comprise two LysM domains bind chitin through intermolecular dimerization

Hui Tian[1], Gabriel L. Fiorin[1], Anja Kombrink[1], Jeroen R. Mesters[2,*], Bart P.H.J. Thomma[1,3,*]

[1]Laboratory of Phytopathology, Wageningen University and Research, Droevendaalsesteeg 1, 6708PB Wageningen, The Netherlands; [2]Institute of Biochemistry, University of Lübeck, Ratzeburger Allee 160, 23538 Lübeck, Germany; [3]University of Cologne, Institute for Plant Sciences, Cluster of Excellence on Plant Sciences (CEPLAS), 50674 Cologne, Germany.

*To whom correspondence should be addressed. E-mail: bart.thomma@wur.nl

SUMMARY

Chitin is a polymer of β-(1,4)-linked *N*-acetyl-D-glucosamine (GlcNAc) and a major structural component of fungal cell walls that acts as a microbe-associated molecular pattern (MAMP) that can be recognized by plant cell surface-localized pattern recognition receptors (PRRs) to activate a wide range of immune responses. In order to deregulate chitin-induced plant immunity and successfully establish their infection, many fungal pathogens secrete effector proteins with LysM domains. We previously determined that two of the three LysM domains of the LysM effector Ecp6 from the tomato leaf mould fungus *Cladosporium fulvum* cooperate to form a chitin-binding groove that binds chitin with ultra-high affinity, allowing to outcompete host PRRs for chitin binding. In this study, we describe functional and structural analyses aimed to investigate whether LysM effectors that contain two LysM domains bind chitin through intramolecular or intermolecular LysM dimerization. To this end, we focus on MoSlp1 from the rice blast fungus *Magnaporthe oryzae*, Vd2LysM from the broad host range vascular wilt fungus *Verticillium dahliae*, and ChElp1 and ChElp2 from the Brassicaceae anthracnose fungus *Colletotrichum higginsianum*. We show that these LysM effectors bind chitin through intermolecular LysM dimerization, allowing the formation of polymeric complexes that may precipitate in order to eliminate the presence of chitin oligomers at infection sites to suppress activation of chitin-induced plant immunity. In this manner, many fungal pathogens are able to subvert chitin-triggered immunity in their plant hosts.

INTRODUCTION

Chitin is a homopolymer of β-(1,4)-linked *N*-acetyl-D-glucosamine (GlcNAc) and a major structural component of fungal cell walls (Free, 2013; Lenardon *et al.*, 2010). Additionally, chitin has been characterized as a fungal microbe-associated molecular pattern (MAMP) that can be recognized by plant cell surface-localized pattern recognition receptors that contain extracellular LysM domains (LysM-PRRs) (Rovenich *et al.*, 2016; Sanchez-Vallet *et al.*, 2015; Zhang *et al.*, 2007; Zipfel, 2008). Upon recognition of chitin by such receptors, plants evoke a broad range of immune responses including the production of reactive oxygen species (ROS), the activation of mitogen-associated protein kinases (MAPKs), the generation of ion fluxes and the expression of defence-related genes that include those encoding hydrolytic enzymes such as chitinases in order to halt fungal invasion (Altenbach and Robatzek, 2007; Boller and Felix, 2009; Felix *et al.*, 1993; Jones and Dangl, 2006; Sanchez-Vallet *et al.*, 2015). LysM-PRRs have been functionally characterized in several plants, including the model plant Arabidopsis (*Arabidopsis thaliana*) in which the LysM receptor AtLYK5 binds chitin with high affinity (1.72 μM) and recruits AtLYK4 and AtCERK1 upon chitin elicitation to form a tripartite receptor complex to initiate chitin signalling (Cao *et al.*, 2014). AtCERK1 was found to bind chitin directly as well, albeit with approximately 200-fold lower affinity than AtLYK5 (Cao *et al.*, 2014; Miya *et al.*, 2007; Petutschnig *et al.*, 2010). Moreover, a crystal structure of the ectodomain of AtCERK1 revealed that only one out of its three LysMs (LysM2) binds chitin (Liu *et al.*, 2012).

To avoid chitin-induced immune responses, successful fungal pathogens evolved various strategies to either protect fungal cell wall chitin against hydrolysis by host enzymes, or prevent the activation of plant immunity by fungal cell wall-derived chitin oligomers (de Jonge *et al.*, 2010; Rovenich *et al.*, 2014; Sanchez-Vallet *et al.*, 2015). A

well-studied fungus for which several strategies to deal with chitin-triggered immunity have been characterized is *Cladosporium fulvum*, the fungus that causes leaf mould disease of tomato. *C. fulvum* secretes the Ecp6 effector protein during host colonization, which contains three LysMs and binds chitin oligosaccharides with ultra-high affinity, to prevent the activation of chitin-induced plant immune responses (Bolton *et al.*, 2008; de Jonge *et al.*, 2010). A crystal structure of Ecp6 revealed that two of its three LysMs cooperate to form a composite chitin-binding groove that binds chitin through intrachain LysM dimerization (Sanchez-Vallet *et al.*, 2013). The genome of another host-specific fungus, *Zymoseptoria tritici*, the causal agent of Septoria tritici blotch (STB) of wheat, encodes a close homolog of Ecp6 known as Mg3LysM that similarly suppresses chitin-triggered immunity (Marshall *et al.*, 2011). Additionally, the *Z. tritici* genome encodes two secreted effectors that carry a single LysM only. Of these, Mg1LysM was characterized to protect hyphae against hydrolysis by plant chitinases (Marshall *et al.*, 2011). An Mg1LysM crystal structure showed that two Mg1LysM monomers form a chitin-independent homodimer via the β-sheet that is present in the *N*-terminus of Mg1LysM (Sánchez-Vallet *et al.*, 2019). Furthermore, Mg1LysM homodimers undergo ligand-induced polymerization in the presence of chitin, leading to a polymeric structure that is able to protect fungal cell walls (Sánchez-Vallet *et al.*, 2019). In contrast to Ecp6 and Mg3LysM, Mg1LysM cannot suppress chitin-triggered immune responses in host plants (Marshall *et al.*, 2011).

Suppression of chitin-triggered immunity by secreted fungal effectors that only carry LysM domains, collectively referred to as LysM effectors, has been demonstrated for various phytopathogenic fungi by now. For instance, *Magnaporthe oryzae*, the causal agent of rice blast disease, secretes the LysM effector Slp1 to bind chitin and suppresses chitin-triggered immune responses (Mentlak *et al.*, 2012). Similarly, the Brassicaceae

anthracnose fungus *Colletotrichum higginsianum* secretes Elp1 and Elp2, while the broad host-range vascular wilt fungus *Verticillium dahliae* secretes Vd2LysM (Kombrink *et al.*, 2017; Takahara *et al.*, 2016). While these examples are from plant-associated Ascomycete fungi, also plant-associated fungi that belong to other phyla utilize LysM effectors to suppress chitin-triggered immunity. For instance, the Basidiomycota soil-borne broad host-range pathogen *Rhizoctonia solani* secretes RsLysM, while the Glomeromycota arbuscular mycorrhizal fungus *Rhizophagus irregularis* secretes RiSLM to suppress chitin-triggered immunity (Dolfors *et al.*, 2019; Zeng *et al.*, 2020). The latter example demonstrates that also non-pathogenic fungi utilize LysM effectors in their interaction with host plants. Moreover, the finding that LysM effectors contribute to the virulence of the Ascomycete fungus *Beauveria bassiana* by evasion of immune responses in insect hosts demonstrates that LysM effectors play roles in fungal interactions beyond plant hosts (Cen *et al.*, 2017; Kombrink and Thomma, 2013). Intriguingly, almost all characterized LysM effectors that were shown to suppress chitin-triggered immunity in plant hosts contain two LysM domains, except for Ecp6 and Mg3LysM that possess three LysMs, and RiSLM that possesses only one LysM.

Based on the functional analysis of *C. fulvum* Ecp6, it has been proposed that the ability to suppress chitin-triggered immunity resides in the ability to bind chitin with ultrahigh affinity, such that host chitin receptors can be outcompeted for substrate binding (Sanchez-Vallet *et al.*, 2013; Sanchez-Vallet *et al.*, 2015). In Ecp6, and most likely also in Mg3LysM, the ultrahigh affinity is mediated by intramolecular LysM dimerization of two of the three LysM domains. However, it remains unclear whether LysM effectors that comprise two LysMs are able to similarly undergo intramolecular LysM dimerization, which then would allow for ultrahigh chitin-binding affinity. Thus, in order to understand how these LysM effectors suppress chitin-triggered immunity, we

110 performed functional and structural analysis using several representatives of this group
111 of LysM effectors, namely MoSlp1 from *M. oryzae*, Vd2LysM from *V. dahliae*, ChElp1 and
112 ChElp2 from *C. higginsianum*.
113
114

RESULTS

Three-dimensional structure prediction of LysM effectors with two LysM domains

It has previously been determined that MoSlp1 from *M. oryzae*, Vd2LysM from *V. dahliae*, and ChElp1 and ChElp2 from *C. higginsianum* contain two LysM domains, bind chitin and suppress chitin-induced host immunity (Kombrink *et al.*, 2017; Mentlak *et al.*, 2012; Takahara *et al.*, 2016). Their length varies from a minimum of 145 aa (Vd2LysM) to a maximum of 176 aa (ChElp2), with the molecular weight of the mature proteins ranging from 14.24 to 16.14 kDa (Fig. 1A). An amino acid sequence alignment of the LysM domains of the LysM effectors with two LysM domains with those of *C. fulvum* Ecp6 displayed a significant conservation of the domains, and of the residues involved in chitin binding in particular (Fig. S1). Structural analysis of Ecp6 has previously revealed that the first and third LysM domain cooperate to form a composite ultra-high affinity chitin-binding groove, enabled by a long and flexible linker between these domains (Sanchez-Vallet *et al.*, 2013). To assess whether intramolecular LysM dimerization could also occur in MoSlp1, Vd2LysM, ChElp1 and ChElp2, their overall three-dimensional structure was predicted using two software packages, I-TASSER and Phyre2 (Kelley *et al.*, 2015; Roy *et al.*, 2010; Yang and Zhang, 2015). Interestingly, the predicted three-dimensional structures by the different methods resulted in protein models with different substrate-binding possibilities (Fig. 2). The four structures modelled by I-TASSER are predicted to have confidence (C) scores of -0.92, -0.86, -0.99 and -0.91 for MoSlp1, Vd2LysM, ChElp1 and ChElp2, respectively on a scale between -5 and 2, where models with C-scores > -1.5 are considered reliable (Roy *et al.*, 2010). It is important to note that the surface-areas with amino-acid residues involved in chitin binding are facing outward in these structures (Fig. 2), and that the linker regions between the two LysM domains are much more tightly packed and thus do not straightforward permit for

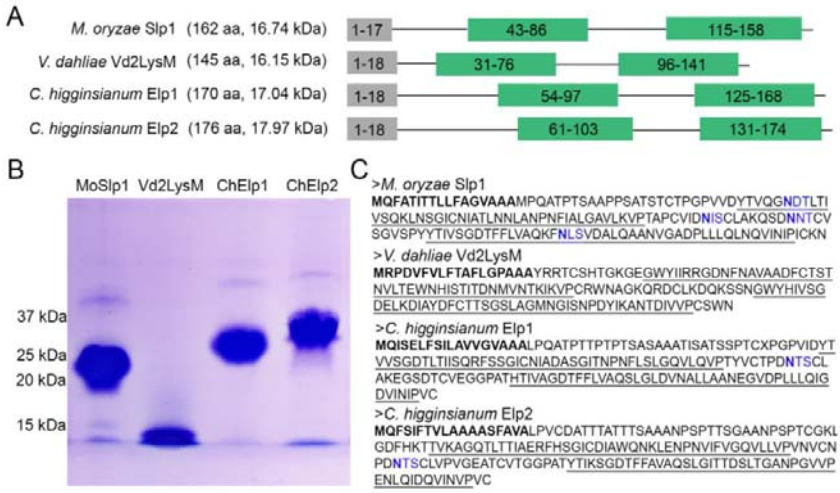

Fig. 1 Characteristics and heterologous production of four LysM effectors. (A) Schematic representation of four fungal LysM effectors that contain two LysM domains. Signal peptides (grey boxes) were predicted with SignalP 4.0 (http://www.cbs.dtu.dk/services/SignalP-4.0/) and LysM domains (green boxes) with InterPro (https://www.ebi.ac.uk/interpro/). The numbers in the boxes indicate the amino acids that compose the motif. (B) Protein polyacrylamide gel electrophoresis of 1 µl of purified and concentrated preparation of the effectors produced in *Pichia pastoris* followed by CBB staining. (C) Primary amino acid sequence of the four LysM effectors with signal peptides in bold, LysMs underlined, and putative *N*-glycosylation sites as predicted with the NetNGlyc 1.0 Server (http://www.cbs.dtu.dk/services/NetNGlyc/) in blue. *N*-glycosylation sites are composed of asparagine-X-Serine/Threonine (N-X-S/T) triads, with the asparagines that may be *N*-glycosylated in bold.

a structural reorganisation of the two domains to enable intramolecular LysM dimerization. In contrast, Phyre2 presents a model where the two LysM domains of

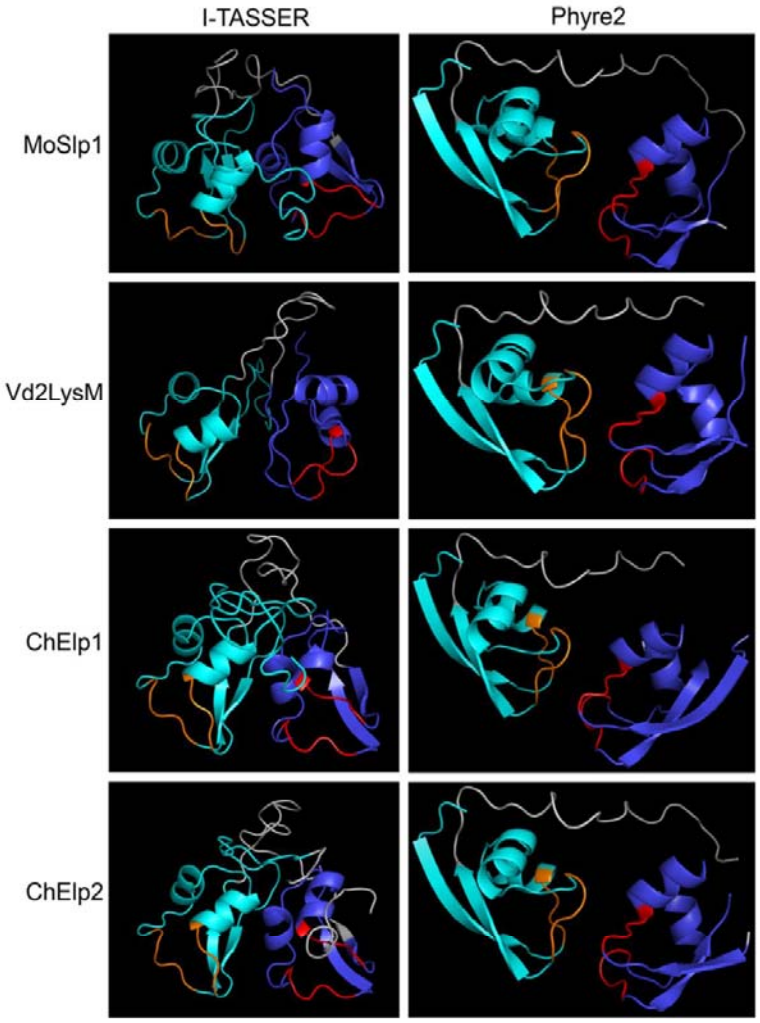

Fig. 2 *In-silico* prediction of the three-dimensional structures of four LysM effectors with two LysM domains with I-TASSER and Phyre2 software. Residues proposed to be involved in chitin binding are indicated in orange and red. Structures were visualized using the PyMOL molecular graphics system (Schrodinger LLC, 2015).

142 MoSlp1 are facing inward and intramolecular LysM dimerization is possible by
143 maximally stretching the linker in between the two LysM domains. However, for the

three additional LysM effectors Phyre2 is only able to allow intramolecular LysM dimerization by interrupting this linker domain, suggesting that intramolecular LysM dimerization is normally not possible. Thus, except for MoSlp1 for which the two software tools disagree, both tools agree that chitin binding through intramolecular dimerization is highly unlikely. Based on these predictions, we decided to further pursue investigations into the substrate-binding mechanisms of fungal effectors that contain two LysM domains.

Heterologous LysM effector production

The most direct method to reveal the chitin-binding mechanism of a LysM effector is by determination of a three-dimensional protein structure in the presence of chitin, for instance by X-ray crystallography. This strategy requires a protein crystal of sufficient size and quality to be used in an X-ray diffraction experiment, which in turn requires highly pure protein of a sufficiently high concentration. To this end, heterologous production of each of the LysM effectors as *N*-terminally 6×His-FLAG-tagged fusion protein was performed using *Pichia pastoris* as a yeast expression system. After purification from the culture filtrate, the LysM effectors were subjected to protein polyacrylamide gel analysis, revealing that only Vd2LysM migrated as expected based on its predicted molecular weight (Fig. 1AB). Interestingly, the three other proteins (MoSlp1, ChElp1 and ChElp2) migrated slower than expected based on their calculated molecular weights (Fig. 1AB), suggesting the presence of post-translational modifications, such as glycan decorations, on these proteins (Haltiwanger and Lowe, 2004; Moremen *et al.*, 2012; Nagashima *et al.*, 2018; Xu and Ng, 2015). On the one hand, however, glycans can greatly hamper crystal packing since they may prevent or reduce favourable molecular contacts between protein molecules. Moreover, glycosylation may

cause microheterogeneity in protein solutions that affects protein ordering as well (Baker *et al.*, 1994; Davis *et al.*, 1993; Tang *et al.*, 2019). On the other hand, glycosylation may be explicitly required for proper protein folding and/or aid in crystal growth by forming critical intermolecular contacts and thus, does not *a priori* hinder crystallization(Mesters *et al.*, 2007).

To assess the potential for posttranslational modifications to occur on LysMs, we performed *N*-linked protein glycosylation site prediction. MoSlp1 was predicted to possess four potential glycosylation sites (**N^{48}**DT, **N^{94}**IS, **N^{130}**LS and **N^{104}**NT) on four asparagine residues (Asn, N) that match the glycosylation consensus sequence Asn-Xaa-Ser/Thr (N-X-S/T), where X can be any amino acid except proline (Pro, P) or glutamate (Glu, E) (Fig. 1C). ChElp1 as well as ChElp2 contains only a single potential glycosylation site, namely **N^{105}**TS and **N^{111}**TS, respectively (Fig. 1C). Consistent with our protein polyacrylamide gel electrophoresis observation, Vd2LysM is not predicted to possess any glycosylation site (Fig. 1C). These predictions were matched by a glycoprotein staining assay, revealing that Vd2LysM is the only one out of the four proteins that does not react with the dye (Fig. S2), and confirming that MoSlp1, ChElp1 and ChElp2 were indeed glycosylated during yeast production.

In an attempt to increase protein homogeneity and possibly promote crystallization success, enzymatic deglycosylation was pursued based on mannosidase treatment. However, treatment of MoSlp1 and ChElp2 with mannosidase failed to decrease the observed molecular weights of the proteins in polyacrylamide gel analysis (Fig. 3), suggesting that high-mannose-type N-glycans do not form the most important glycan decorations on these proteins. To further pursue enzymatic deglycosylation of the LysM proteins, the peptide:N-glycosidase F (PNGase F) amidase that cleaves between the innermost GlcNAc and asparagine residues of high mannose, hybrid, and

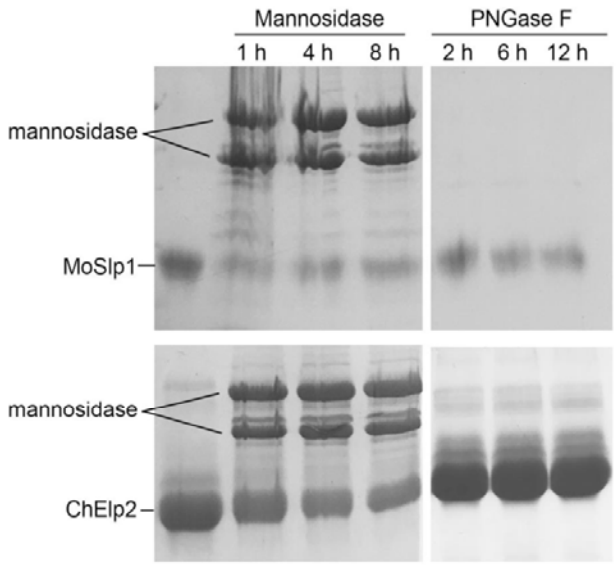

Fig. 3 Treatment of the *P. pastoris*-produced LysM effectors MoSlp1 and ChElp2 with mannosidase and PNGase F in an attempt to remove putative *N*-glycans. Polyacrylamide gel electrophoresis of the LysM effectors MoSlp1 (top panels) and ChElp2 (bottom panels) after incubation with mannosidase (left panels) and PNGase F (right panels). Protein samples were collected at different time points after incubation and subjected to gel electrophoresis followed by CBB staining.

194 complex oligosaccharides from N-linked glycoproteins was used on MoSlp1 and ChElp2.

195 Unfortunately, also this treatment did not decrease the observed molecular weights (Fig.

196 3).

197 As an alternative strategy to reduce glycosylation of the protein preparations,
198 site-directed mutagenesis was conducted on *ChElp1* and *ChElp2* such that the
199 asparagines in the single potential glycosylation sites, **N^{105}** and **N^{111}** respectively, were
200 replaced by glutamines (Gln, Q). Unfortunately, however, production of the mutated
201 proteins failed repeatedly due to protein instability. As we have previously successfully
202 crystallized Ecp6 protein that was produced in the same manner despite containing two
203 spatially close glycosylation sites that were indeed found to be glycosylated in the
204 crystal structure (Sanchez-Vallet *et al.*, 2013), we decided to arrest our efforts to prevent
205 glycosylation of the proteins.

206

207 **Solubility and homogeneity of the LysM protein preparations**

208 Since the isoelectric point (pI) is an important indicator of protein solubility, the pI of
209 the four proteins was calculated. Whereas MoSlp1, ChElp1 and ChElp2 were determined
210 to be acidic proteins with pI of 4.48, 3.73 and 4.64, respectively, Vd2LysM was calculated
211 to have a rather neutral pI of 7.76. Based on the pIs, all four LysM proteins were
212 dissolved in a buffer with pH 8.5 (20 mM Tris, 150 mM NaCl, 5% glycerol), and
213 concentrated (>7 mg/mL) without occurrence of visible precipitation (Table S1).

214 Next, dynamic light scattering (DLS) was employed to determine the molecular
215 homogeneity of the protein solutions (Dessau and Modis, 2011; Proteau *et al.*, 2010).
216 The DLS heatmaps exhibited extremely heterogenous particle size distributions for each
217 of the LysM proteins. In particular, the particle size distribution for MoSlp1 and ChElp2
218 was quite heterogenous and ranged from 10 nm to 100 nm (Fig. 4A), which is
219 significantly larger than the expected size of 1-3 nm for a protein with a molecular
220 weight of approximately 16 kDa. Although less heterogenous, ChElp1 mostly occurred as

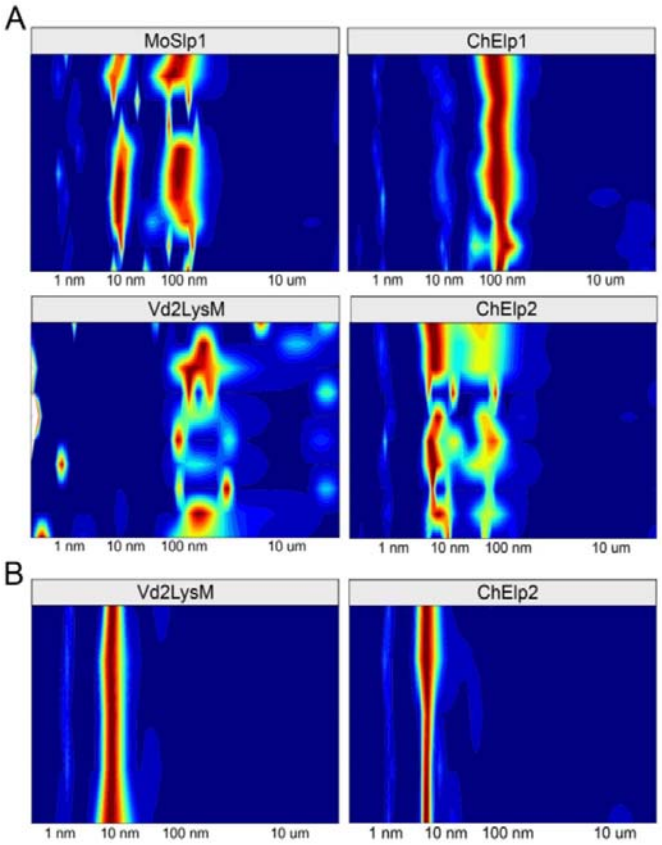

Fig. 4 Particle size distribution of four LysM effectors as measured by dynamic light scattering (DLS). The particle size distribution is shown as a colour scale heat map ranging from blue (lowest abundance) to red (highest abundance) for a particle size range of 1 nm to 100 µM. (A) Heat maps of the four *Pichia pastoris*-produced LysM effectors after initial purification and concentration. (B) Heat maps of Vd2LysM and ChElp2 after gel filtration and decyl β-D-maltopyranoside (DM) treatment.

221 particles of around at 100 nm, which again points towards a significant degree of
222 aggregation (Fig. 4A). Finally, Vd2LysM occurred as a heterogenous population of

223 particles of 100 nm and larger. The heterogeneity of the four protein preparations
224 together with the relatively large particle size is likely to negatively impact crystal
225 formation (Niesen *et al.*, 2008; Price 2nd *et al.*, 2009).

226 In order to improve protein solubility and particle size distribution, gel filtration
227 and mild detergent treatment were pursued for all four LysM effectors. However,
228 eventually, we only successfully improved the homogeneity of Vd2LysM and ChElp2 by
229 gel filtration combined with the treatment with the nonionic detergent decyl β-D-
230 maltopyranoside (DM). These protein samples were tested by DLS, which revealed
231 uniform particle distributions for both proteins with main molecular populations at
232 around 10 nm (Fig. 4B). Therefore, both protein preparations were used for
233 crystallization screenings.

234

235 **Attempts to obtain protein crystals failed for all four LysM effectors**

236 Primary protein crystallization is a screening experiment where a concentrated solution
237 of target protein is subjected to a variety of conditions that cover a wide range of buffers,
238 salts, precipitating agents, pH, additives and even ligands (Bergfors, 2009; Chayen and
239 Saridakis, 2008; Skarina *et al.*, 2014). The ultimate aim is to reach a protein's supersaturation
240 state, where protein molecules may self-assemble into a periodically repeating pattern that
241 extends in three dimensions, yielding protein crystals. For protein crystallization, there is
242 no systematic analysis or comprehensive theory to guide efforts to directions that can
243 increase the success rate. Consequently, macromolecular crystal growth largely remains
244 empirical (McPherson and Gavira, 2014). Both structures of *C. fulvum* Ecp6 and *Z. tritici*
245 Mg1LysM were determined using protein crystals obtained from *P. pastoris*-produced
246 protein preparations without additional chitin treatment. However, chitin molecules were
247 found to be already present in the Ecp6 and Mg1LysM crystals, suggesting that they were

derived from the cell wall of yeast. In this study, four *P. pastoris*-produced LysM proteins were directly subjected to initial screening using commercial crystallization kits PACT premier™, Salt^{RX}, Index^{TM}, PEG^{RX} and PEG/Ion screen (96 conditions/kit) with the original concentrations (Table S1). Because we observed instant heavy precipitations in more than half of the conditions, the four LysM protein preparations were diluted to half the original concentrations and subjected to the initial screening again. Unfortunately, none of these attempts yielded any genuine protein crystals. Subsequently, we pre-incubated the LysM proteins with chitinhexaose in molar ratios of 3:1 and 1:1 (protein:chitin) and subjected them to the initial crystallization screening again. However, even after one year, none of the conditions developed genuine protein crystals.

To promote crystallization, active small molecules, traditionally referred to as "additives", can be added to promote the formation of favourable lattice contacts (McPherson *et al.*, 2011; McPherson and Cudney, 2006). Therefore, we conducted further screenings by adding 96 additives into two different buffers, namely i) 0.1 M HEPES, 30% PEG 3350, pH 7.0; ii) 50%Tacsimate, which is a mixture of organic acids with pH 7.0, for all four LysM proteins at their original concentrations as well as at half-diluted concentrations. Unfortunately, none of these attempts yielded any genuine protein crystals.

Finally, Vd2LysM and ChElp2 were produced in *E. coli* and subjected to an initial screening in the absence of exogenously added chitin and after pre-treatment with chitinhexaose in molar ratios of 3:1 and 1:1 (protein:chitin) using the five commercial kits, and also subjected to the additive screen kit in the two different buffers. Unfortunately, also these attempts were in vain.

Chitin-induced polymerisation suggests intramolecular LysM dimerization

As all our crystallization attempts for the four different LysM effectors failed, we pursued other strategies to provide evidence for the occurrence of either inter- or intramolecular LysM dimerization. We reasoned that treatment with chitin oligomers would lead to higher order oligomeric or polymeric protein complexes if intermolecular LysM dimerization occurs (Fig. 5, hypothesis I), while such complexes will not be formed in case of intramolecular LysM dimerization (Fig. 5, hypothesis II). To address these hypotheses, ChElp2 was selected as a representative and was expressed in *Escherichia coli* to obtain protein that is devoid of chitin. After purification and concentration, the aggregation status of the two protein preparations was tested with DLS. Interestingly, the addition of chitin resulted in a clear shift in particle size distribution in a concentration-dependent manner. Whereas a 3:1 protein:chitin molecular ratio shifted the particle size distribution of ChElp2 towards larger complexes of 10 nm to 100 nm (Fig. 6), further addition of chitin to a protein:chitin ratio of 1:1 fully shifted the dominant ChElp2 particle size towards 100 nm (Fig. 6). This finding strongly suggests that chitin addition mediates intermolecular LysM dimerization, leading to the formation of polymeric protein complexes.

As a second, independent line of evidence for polymerization, we hypothesized that if ChElp2 undergoes chitin-induced polymerization, we should be able to precipitate polymeric complexes during centrifugation. Thus, with Ecp6 as a negative control, we incubated ChElp2 overnight with chitohexaose and subsequently centrifuged the samples at 20,000 g in the presence of 0.002% methylene blue to visualize the protein. Indeed, a clear protein pellet appeared when ChElp2 was incubated with chitin, but not in the control treatment without chitin, nor in the Ecp6 samples (Fig. 7). Next, we

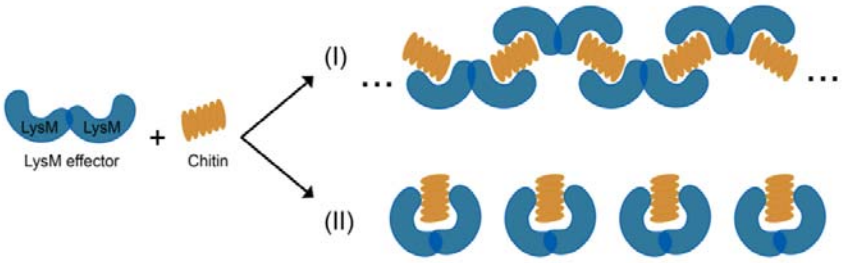

Fig. 5 Two hypotheses for chitin binding by fungal effectors containing two LysM domains. LysM effectors that contain two LysMs may bind chitin through (I) intermolecular dimerization, which should not lead to polymerisation, or through (II) intramolecular dimerization, in which LysM effectors may undergo ligand-induced polymerization.

295 assessed whether a similar precipitation in the presence of chitin, as evidence for
296 polymerisation, could be obtained for MoSlp1 and Vd2LysM as well. Indeed, this appeared

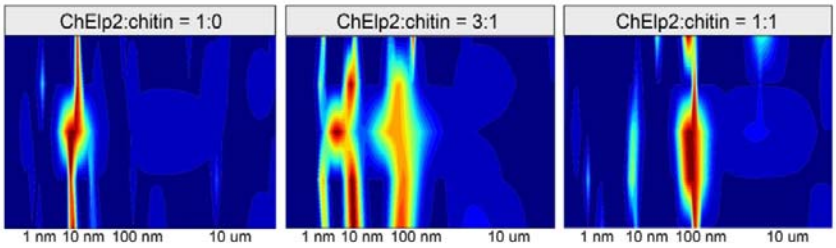

Fig. 6 Particle size distribution of ChElp2 in absence and presence of chitin as measured by dynamic light scattering (DLS). The particle size distribution is shown as a colour scale heat map ranging from blue (lowest abundance) to red (highest abundance) for a particle size range of 1 nm to 100 μM.

297 to be the case (Fig. 7). Collectively, these data confirm the occurrence of chitin-induced
298 polymerisation of LysM effectors that comprise two LysMs, and prove that

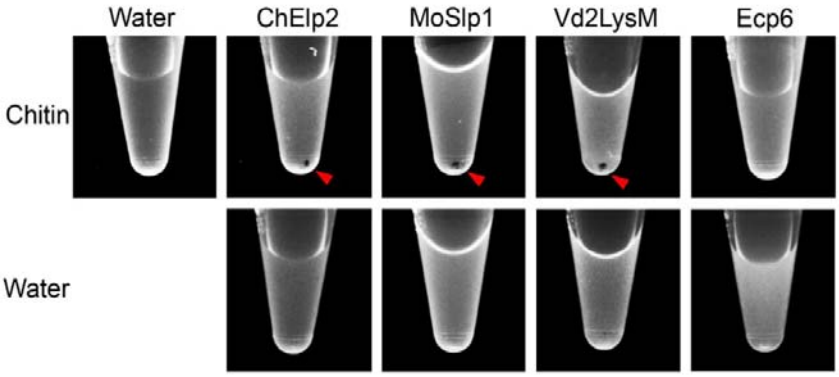

Fig. 7 Chitin-induced polymerization of LysM effectors with two LysM domains. The LysM effector proteins ChElp2, MoSlp1 and Vd2LysM, together with Ecp6 as negative control, were incubated with chitohexaose (chitin) or water. After overnight incubation, methylene blue was added and protein solutions were centrifuged, resulting in protein pellets (red arrowheads) as a consequence of polymerization for ChElp2, MoSlp1 and Vd2LysM, but not for Ecp6.

299 intermolecular dimerization (Fig. 5, hypothesis I) rather than intramolecular
300 dimerization (Fig. 5, hypothesis II) occurs in the presence of chitin.

301

302

DISCUSSION

To address the question whether LysM effectors that comprise two LysM domains bind chitin through inter- or intramolecular dimerization, we heterologously expressed four such LysM proteins and pursued the determination of 3D-protein structures based on X-ray crystallography. We screened the four *P. pastoris*-produced LysM effectors in two different concentrations with five different commercial kits that amount to a total of 480 conditions, in absence and presence of chitin in two different ratios, as well as with an additive screening in two different buffers with a total of 192 conditions. Moreover, for Vd2LysM and ChElp2, *E. coli*-produced protein was screened under the above-mentioned conditions as well. Although we tested this large amount of conditions on four homologous proteins, no protein crystals developed. Generally, if crystallization of a protein fails, it can be attributed to many factors, ranging from insufficient purity and homogeneity of the protein, to the fact that some proteins are simply naturally or biologically unable to crystalize (Dessau and Modis, 2011; Wlodawer *et al.*, 2017). In this study, we tried to address as many factors with respect to protein quality as possible, but our attempts to obtain protein crystals failed nonetheless.

Obviously, absence of crystal formation does not prove that crystal formation is impossible. However, the lack of crystal formation inspired our further thoughts about LysM effector chitin binding. Theoretically, we anticipated that two possible substrate-binding mechanisms may occur for our LysM effectors (Fig. 5): chitin binding through inter- (hypothesis I) or intramolecular (hypothesis II) chitin binding. If intramolecular chitin binding would occur, it can be expected that chitin molecules reduce protein flexibility and promote protein homogeneity in solution, theoretically promoting crystal formation. However, arguably, if intermolecular chitin binding is prevalent, polymerization is likely to occur, which may involve chains of polymers of variable

lengths. As a consequence, homogeneity in protein solution may be severely compromised, leading to precipitation rather than to crystallization. The finding that exogenously added chitin can induce the formation of oligomeric complexes of ChElp2 as determined in DLS experiments (Fig. 6) suggested that oligomers indeed occur, pointing towards the occurrence of intermolecular dimerization as proposed in hypothesis I (Fig. 5). However, solid proof was subsequently obtained by performing centrifugation experiments upon incubation with chitin hexamers, revealing that protein pellets as a consequence of chitin-induced polymerisation were obtained not only for ChElp2, but also for MoSlp1 and VdLysM2 (Fig. 7). The finding that such pellets were not obtained with Ecp6 is important, as it demonstrates that the pellets are associated with intermolecular dimerization of LysM effector molecules, a process that is not supposed to occur with Ecp6 that undergoes intramolecular LysM dimerization (Sanchez-Vallet *et al.*, 2013).

The initial prediction of the three-dimensional protein structures with I-TASSER as well as with Phyre2 could not support the occurrence of intramolecular dimerization of LysMs to mechanistically explain chitin binding by LysM effectors that comprise two LysMs. Our experimental evidence further supports this notion. Taken together, we propose that fungal LysM effectors that comprise two LysM domains bind chitin through intermolecular dimerization, contributing to fungal virulence through formation of polymeric complexes that have the propensity to precipitate in order to eliminate the presence of chitin oligomers at infection sites that may otherwise alarm the host immune system.

MATERIALS AND METHODS

Sequence alignment and three-dimensional protein structure prediction

LysM domains of proteins were predicted by InterPro (https://www.ebi.ac.uk/interpro/; Finn *et al.*, 2017) and the alignment of amino acid sequences was performed by ClustalX2. Protein structures were predicted with I-TASSER (https://zhanglab.ccmb.med.umich.edu/I-TASSER/; Roy *et al.*, 2010) and with Phyre2 (http://www.sbg.bio.ic.ac.uk/~phyre2/html/page.cgi?id=index; Kelley *et al.*, 2015). Structures were viewed by the PyMOL molecular graphics system, version 2 (Schrodinger LLC, 2015).

Heterologous protein production in *Pichia pastoris*

Protein sequences were analysed using SignalP4.0 (http://www.cbs.dtu.dk/services/SignalP; Petersen *et al.*, 2011) and the coding sequences of mature proteins without signal peptide were amplified with primers listed in Table S2, fused with an N-terminal 6×His-tag and cloned into expression vector pPIC9 (Thermo Fisher Scientific, California, USA). Correctness of the resulting constructs was confirmed by DNA sequencing prior to introduction into *Pichia pastoris* strain GS115 (Thermo Fisher Scientific, California, USA). Fermentation was conducted in approximately 3 L of culture in a bioreactor BioFlo120 (Eppendorf, Hamburg, Germany) at 30°C for 5 days, including 3 days of methanol induction. Next, *P. pastoris* cells were pelleted by centrifugation at 3800 g at 4°C for 50 min and the supernatant was concentrated to 200 ml using a Vivaflow 200 Cross Flow Cassette (5000NWCO; Sartorius, Göttingen, Germany) at 4°C for approximately 20 h. The concentrated supernatant was purified using His60 Ni Superflow resin (TaKaRa, California, USA) on a BioLogic LP system (Bio-Rad, California, USA). Purified protein was analysed by protein

polyacrylamide gel electrophoresis followed by staining with Coomassie Brilliant Blue (CBB) and dialyzed against 5 L of 50 mM Tris, 150 mM NaCl to remove imidazole. Finally, proteins were further concentrated using Amicon Ultra-15 Centrifugal Filter Units (MERCK, Carrigtohill, Ireland) and stored at -20°C.

Heterologous protein production in *E. coli*

Coding sequences of mature proteins without signal peptide were amplified with primers listed in Table S2 and cloned into expression vector pETSUMO (Thermo Fisher Scientific, Massachusetts, USA). Correctness of the resulting constructs pETSUMO-ChElp2 and pETSUMO-Vd2LysM were confirmed by DNA sequencing and introduced into *E. coli* strains BL21 and Origami, respectively. Both proteins were produced at 28°C with 0.2 mM IPTG. Cell culture was pelleted by centrifugation at 4000 g for 40 min at 4°C, and the pellet was resuspended in 20 mL lysis buffer (Table S2), shaken at 4°C for at least two hours and centrifuged at 10,000 g for 1 h. The supernatant was collected and purified using His60 Ni Superflow resin (TaKaRa, California, USA) on a BioLogic LP system (Bio-Rad, California, USA). The resulting protein was dialyzed 3 L of 20 mM Tris, 150 mM NaCl, 5 % glycerol, pH 8.0 while 5 µL of cleavage protein ULP1 was added into the dialysis membrane to cleave-off the 6×His-SUMO tag. Next day, protein solution was collected and subjected to purification using His60 Ni Superflow resin (TaKaRa, California, USA) to remove 6×His-SUMO tag from the protein preparations. Eventually, LysM proteins were dissolved in 20 mM Tris, 150 mM NaCl, 5% glycerol, pH 8.0 and concentrated to a high concentration.

399 **Glycoprotein staining assay**

400 1 µL of concentrated LysM protein solution was tested using a protein polyacrylamide
401 gel followed by CBB and glycoprotein staining with the Pierce Glycoprotein Staining Kit
402 (Thermo Fisher Scientific, California, USA) according to the manufacturer's instructions,
403 including the addition of horseradish peroxidase and soybean trypsin inhibitor as
404 positive and negative control, respectively.

405

406 **Mannosidase and PNGase F treatments**

407 Deglycosylation was conducted with α-Mannosidase from *Canavalia ensiformis* (MERCK,
408 New Jersey, USA) and PNGase F (MERCK, New Jersey, USA) according to the
409 manufacturer's instructions. 5 µl of concentrated LysM protein solution was treated
410 with 10 µl of α-mannosidase (1 mg/ml, pH 4.5) at 25°C or 1 µl PNGase F (one unit, pH 7.5)
411 at 37°C. Protein samples were collected after 1, 4 and 8 h of incubation for α-
412 mannosidase treatment, and after 2, 6 and 12 h of incubation for PNGase F treatment.
413 Subsequently, protein samples were analysed using protein polyacrylamide gel
414 electrophoresis followed by CBB staining.

415

416 **Crystallization conditions**

417 Commercial kits PACT premier™ (Molecular dimensions, Sheffield, UK) and Salt^{RX},
418 Index^{TM}, Shotgun, PEG^{RX}, PEG/Ion screen (Hampton Research, California, USA) were
419 used for initial screening. 96-well protein crystallization plates were prepared using a
420 Crystal Phoenix robot (Art Robbins Instruments, California, USA). Chitohexaose
421 (Megazyme, Wicklow, Ireland) was added in molar ratios of 3:1 and 1:1. The additive
422 screening was conducted using the Additive Screen HR2-428 (Hampton Research,

California, USA) and Tacsimate pH 7.0 (Hampton Research, California, USA) according to the manufacturer's instructions.

Dynamic light scattering (DLS) measurements

LysM proteins were dialyzed overnight against 100 mM NaCl and used for particle size distribution measurement using a SpectroSize 300 machine (Xtal Concepts, Hamburg, Germany). For the chitin-induced polymerization measurements, proteins were dissolved in 20 mM Tris, 150 mM NaCl, pH 8.0 and treated with 0.1 % Triton X-100. Chitohexaose (Megazyme, Wicklow, Ireland) was added in molar ratios of 1:1 and 1:2 (protein:chitin) and incubated for 4 hours.

Polymerization assay

LysM effector proteins were adjusted to a concentration of 200 µM and 200 µL of each protein was incubated with 200 µL of 2 mM chitohexaose (Megazyme, Wicklow, Ireland), or 200 µL water as control, at room temperature overnight. The next day, 2 µL of 0.2% methylene blue (Sigma-Aldrich, Missouri, USA) was added and incubated for 30 min after which protein solutions were centrifuged at 20,000 g for 15 min. Photos were taken with a ChemiDoc MP system (Bio-Rad, California, USA) with custom setting for RFP.

ACKNOWLEDGEMENT

H. Tian acknowledges receipt of a PhD fellowship from the China Scholarship Council (CSC). Work in the laboratory of B.P.H.J. Thomma is supported by the Research Council for Earth and Life Science (ALW) of the Netherlands Organization for Scientific Research (NWO) and by the Deutsche Forschungsgemeinschaft (DFG, German Research

448 Foundation) under Germany´s Excellence Strategy – EXC 2048/1 – Project ID:
449 390686111. The authors acknowledge support from the partners of the European
450 Research Area Network for Coordinating Action in Plant Sciences (ERA-CAPS)
451 consortium “SIPIS”.

452

453 **AUTHOR CONTRIBUTIONS**

454 HT, JRM, BPHJT conceived the study; HT designed experiments; HT, GLF and AK
455 performed experiments; HT analyzed data and wrote the manuscript; JRM and BPHJT
456 supervised the project; all authors discussed the results and contributed to the final
457 manuscript.

458

459 **CONFLICT OF INTEREST**

460 The authors declare no conflict of interest exists.

FIGURE LEGENDS

Fig. 1 Characteristics and heterologous production of four LysM effectors. (A) Schematic representation of four fungal LysM effectors that contain two LysM domains. Signal peptides (grey boxes) were predicted with SignalP 4.0 (http://www.cbs.dtu.dk/services/SignalP-4.0/) and LysM domains (green boxes) with InterPro (https://www.ebi.ac.uk/interpro/). The numbers in the boxes indicate the amino acids that compose the motif. (B) Protein polyacrylamide gel electrophoresis of 1 µl of purified and concentrated preparation of the effectors produced in *Pichia pastoris* followed by CBB staining. (C) Primary amino acid sequence of the four LysM effectors with signal peptides in bold, LysMs underlined, and putative *N*-glycosylation sites as predicted with the NetNGlyc 1.0 Server (http://www.cbs.dtu.dk/services/NetNGlyc/) in blue. *N*-glycosylation sites are composed of asparagine-X-Serine/Threonine (N-X-S/T) triads, with the asparagines that may be *N*-glycosylated in bold.

Fig. 2 *In-silico* prediction of the three-dimensional structures of four LysM effectors with two LysM domains with I-TASSER and Phyre2 software. Residues proposed to be involved in chitin binding are indicated in orange and red. Structures were visualized using the PyMOL molecular graphics system (Schrodinger LLC, 2015).

Fig. 3 Treatment of the *P. pastoris*-produced LysM effectors MoSlp1 and ChElp2 with mannosidase and PNGase F in an attempt to remove putative *N*-glycans. Polyacrylamide gel electrophoresis of the LysM effectors MoSlp1 (top panels) and ChElp2 (bottom panels) after incubation with mannosidase (left panels) and PNGase F (right panels). Protein samples were collected at different time points after incubation and subjected to gel electrophoresis followed by CBB staining.

Fig. 4 Particle size distribution of four LysM effectors as measured by dynamic light scattering (DLS). The particle size distribution is shown as a colour scale heat map ranging from blue (lowest abundance) to red (highest abundance) for a particle size range of 1 nm to 100 µM. (A) Heat maps of the four *Pichia pastoris*-produced LysM effectors after initial purification and concentration. (B) Heat maps of Vd2LysM and ChElp2 after gel filtration and decyl β-D-maltopyranoside (DM) treatment.

Fig. 5 Two hypotheses for chitin binding by fungal effectors containing two LysM domains. LysM effectors that contain two LysMs may bind chitin through (I) intermolecular dimerization, which should not lead to polymerisation, or through (II) intramolecular dimerization, in which LysM effectors may undergo ligand-induced polymerization.

Fig. 6 Particle size distribution of ChElp2 in absence and presence of chitin as measured by dynamic light scattering (DLS). The particle size distribution is shown as a colour scale heat map ranging from blue (lowest abundance) to red (highest abundance) for a particle size range of 1 nm to 100 µM.

Fig. 7 Chitin-induced polymerization of LysM effectors with two LysM domains. The LysM effector proteins ChElp2, MoSlp1 and Vd2LysM, together with Ecp6 as negative control, were incubated with chitohexaose (chitin) or water. After overnight incubation, methylene blue was added and protein solutions were centrifuged, resulting in protein pellets (red arrowheads) as a consequence of polymerization for ChElp2, MoSlp1 and Vd2LysM, but not for Ecp6.

Parsed Citations

Altenbach, D. and Robatzek, S. (2007) Pattern recognition receptors: from the cell surface to intracellular dynamics. Mol. Plant-Microbe Interact. 20, 1031–1039.
Pubmed: Author and Title
Google Scholar: Author Only Title Only Author and Title

Baker, H.M., Day, C.L., Norris, G.E. and Baker, E.N. (1994) Enzymatic deglycosylation as a tool for crystallization of mammalian binding proteins. Acta Crystallogr D Biol Crystallogr 50, 380–384.
Pubmed: Author and Title
Google Scholar: Author Only Title Only Author and Title

Boller, T. and Felix, G. (2009) A renaissance of elicitors: perception of microbe-associated molecular patterns and danger signals by pattern-recognition receptors. Annu. Rev. Plant Biol. 60, 379–406.
Pubmed: Author and Title
Google Scholar: Author Only Title Only Author and Title

Bolton, M.D., Esse, H.P. Van, Vossen, J.H., et al. (2008) The novel Cladosporium fulvum lysin motif effector Ecp6 is a virulence factor with orthologues in other fungal species. Mol. Microbiol. 69, 119–136.
Pubmed: Author and Title
Google Scholar: Author Only Title Only Author and Title

Cao, Y., Liang, Y., Tanaka, K., Nguyen, C.T., Jedrzejczak, R.P., Joachimiak, A. and Stacey, G. (2014) The kinase LYK5 is a major chitin receptor in Arabidopsis and forms a chitin-induced complex with related kinase CERK1. Elife 3, e03766.
Pubmed: Author and Title
Google Scholar: Author Only Title Only Author and Title

Cen, K., Li, B., Lu, Y., Zhang, S. and Wang, C. (2017) Divergent LysM effectors contribute to the virulence of Beauveria bassiana by evasion of insect immune defenses. PLOS Pathog. 13, e1006604.
Pubmed: Author and Title
Google Scholar: Author Only Title Only Author and Title

Chayen, N.E. and Saridakis, E. (2008) Protein crystallization: from purified protein to diffraction-quality crystal. Nat. Methods 5, 147–153.
Pubmed: Author and Title
Google Scholar: Author Only Title Only Author and Title

Davis, S.J., Puklavec, M.J., Ashford, D.A., Harlos, K., Jones, E.Y., Stuart, D.I. and Williams, A.F. (1993) Expression of soluble recombinant glycoproteins with predefined glycosylation: application to the crystallization of the T-cell glycoprotein CD2. Protein Eng 6, 229–232.
Pubmed: Author and Title
Google Scholar: Author Only Title Only Author and Title

Dessau, M.A. and Modis, Y. (2011) Protein crystallization for X-ray crystallography. J Vis Exp 16, 2285.
Pubmed: Author and Title
Google Scholar: Author Only Title Only Author and Title

Dolfors, F., Holmquist, L., Dixelius, C. and Tzelepis, G. (2019) A LysM effector protein from the basidiomycete Rhizoctonia solani contributes to virulence through suppression of chitin-triggered immunity. Mol. Genet. Genomics 294, 1211–1218.
Pubmed: Author and Title
Google Scholar: Author Only Title Only Author and Title

Felix, G., Regenass, M. and Boller, T. (1993) Specific perception of subnanomolar concentrations of chitin fragments by tomato cells: Induction of extracellular alkalinization, changes in protein phosphorylation, and establishment of a refractory state. Plant J. 4, 307–316.
Pubmed: Author and Title
Google Scholar: Author Only Title Only Author and Title

Finn, R.D., Attwood, T.K., Babbitt, P.C., et al. (2017) InterPro in 2017-beyond protein family and domain annotations. Nucleic Acids Res. 45, D190–D199.
Pubmed: Author and Title
Google Scholar: Author Only Title Only Author and Title

Free, S.J. (2013) Fungal cell wall organization and biosynthesis. Adv. Genet. 81, 33–82.
Pubmed: Author and Title
Google Scholar: Author Only Title Only Author and Title

Haltiwanger, R.S. and Lowe, J.B. (2004) Role of glycosylation in development. Annu. Rev. Biochem. 73, 491–537.
Pubmed: Author and Title
Google Scholar: Author Only Title Only Author and Title

Jones, J.D.G. and Dangl, J.L. (2006) The plant immune system. Nature 444, 323–329.
Pubmed: Author and Title
Google Scholar: Author Only Title Only Author and Title

Jonge, R. de, Peter van Esse, H., Kombrink, A., et al. (2010) Conserved Fungal LysM Effector Ecp6 Prevents Chitin-Triggered Immunity in Plants. Science (80-.). 329, 953–955.
Pubmed: Author and Title
Google Scholar: Author Only Title Only Author and Title

Kelley, L.A., Mezulis, S., Yates, C.M., Wass, M.N. and Sternberg, M.J.E. (2015) The Phyre2 web portal for protein modeling, prediction and analysis. Nat. Protoc. 10, 845–858.
Pubmed: Author and Title
Google Scholar: Author Only Title Only Author and Title

Kombrink, A., Rovenich, H., Shi-Kunne, X., et al. (2017) Verticillium dahliae LysM effectors differentially contribute to virulence on plant hosts. Mol. Plant Pathol. 18, 596–608.
Pubmed: Author and Title
Google Scholar: Author Only Title Only Author and Title

Kombrink, A. and Thomma, B.P.H.J. (2013) LysM effectors: secreted proteins supporting fungal life. PLOS Pathog. 9, e1003769.
Pubmed: Author and Title
Google Scholar: Author Only Title Only Author and Title

Lenardon, M.D., Munro, C.A. and Gow, N.A. (2010) Chitin synthesis and fungal pathogenesis. Curr. Opin. Microbiol. 13, 416–423.
Pubmed: Author and Title
Google Scholar: Author Only Title Only Author and Title

Liu, T., Liu, Z., Song, C., et al. (2012) Chitin-induced dimerization activates a plant immune receptor. Science (80-.). 336, 1160–1164.
Pubmed: Author and Title
Google Scholar: Author Only Title Only Author and Title

Marshall, R., Kombrink, A., Motteram, J., Loza-Reyes, E., Lucas, J., Hammond-Kosack, K.E., Thomma, B.P.H.J. and Rudd, J.J. (2011) Analysis of two in planta expressed LysM effector homologs from the fungus Mycosphaerella graminicola reveals novel functional properties and varying contributions to virulence on wheat. Plant Physiol. 156, 756–769.
Pubmed: Author and Title
Google Scholar: Author Only Title Only Author and Title

McPherson, A. and Cudney, B. (2006) Searching for silver bullets: an alternative strategy for crystallizing macromolecules. J Struct Biol 156, 387–406.
Pubmed: Author and Title
Google Scholar: Author Only Title Only Author and Title

McPherson, A. and Gavira, J.A. (2014) Introduction to protein crystallization. Acta Crystallogr F Struct Biol Commun 70, 2–20.
Pubmed: Author and Title
Google Scholar: Author Only Title Only Author and Title

McPherson, A., Nguyen, C., Cudney, R. and Larson, S.B. (2011) The role of small molecule additives and chemical modification in protein crystallization. Cryst. Growth Des. 11, 1469–1474.
Pubmed: Author and Title
Google Scholar: Author Only Title Only Author and Title

Mentlak, T.A., Kombrink, A., Shinya, T., et al. (2012) Effector-Mediated Suppression of Chitin-Triggered Immunity by Magnaporthe oryzae Is Necessary for Rice Blast Disease. Plant Cell 24, 322–335.
Pubmed: Author and Title
Google Scholar: Author Only Title Only Author and Title

Mesters, J.R., Henning, K. and Hilgenfeld, R. (2007) Human glutamate carboxypeptidase II inhibition: structures of GCPII in complex with two potent inhibitors, quisqualate and 2-PMPA. Acta Crystallogr. D. Biol. Crystallogr. 63, 508–513.
Pubmed: Author and Title
Google Scholar: Author Only Title Only Author and Title

Miya, A., Albert, P., Shinya, T., et al. (2007) CERK1, a LysM receptor kinase, is essential for chitin elicitor signaling in Arabidopsis. Proc Natl Acad Sci U S A 104, 19613–19618.
Pubmed: Author and Title
Google Scholar: Author Only Title Only Author and Title

Moremen, K.W., Tiemeyer, M. and Nairn, A. V (2012) Vertebrate protein glycosylation: diversity, synthesis and function. Nat. Rev. Mol. Cell Biol. 13, 448–462.
Pubmed: Author and Title
Google Scholar: Author Only Title Only Author and Title

Nagashima, Y., Schaewen, A. von and Koiwa, H. (2018) Function of N-glycosylation in plants. Plant Sci. 274, 70–79.
Pubmed: Author and Title
Google Scholar: Author Only Title Only Author and Title

Niesen, F.H., Koch, A., Lenski, U., Harttig, U., Roske, Y., Heinemann, U. and Peter, K. (2008) An approach to quality management in structural biology : Biophysical selection of proteins for successful crystallization. 162, 451–459.
Pubmed: Author and Title
Google Scholar: Author Only Title Only Author and Title

Petersen, T.N., Brunak, S., Heijne, G. von and Nielsen, H. (2011) SignalP 4.0: discriminating signal peptides from transmembrane regions. Nat. Methods 8, 785–786.
Pubmed: Author and Title
Google Scholar: Author Only Title Only Author and Title

Petutschnig, E.K., Jones, A.M.E., Serazetdinova, L., Lipka, U. and Lipka, V. (2010) The Lysin Motif Receptor-like Kinase (LysM-RLK) CERK1 is a major chitin-binding protein in Arabidopsis thaliana and subject to chitin-induced phosphorylation. J. Biol. Chem. 285, 28902–28911.
Pubmed: Author and Title
Google Scholar: Author Only Title Only Author and Title

Price 2nd, W.N., Chen, Y., Handelman, S.K., et al. (2009) Understanding the physical properties that control protein crystallization by analysis of large-scale experimental data. Nat. Biotechnol. 27, 51–57.
Pubmed: Author and Title
Google Scholar: Author Only Title Only Author and Title

Proteau, A., Shi, R. and Cygler, M. (2010) Application of dynamic light scattering in protein crystallization. Curr Protoc Protein Sci Chapter 17, Unit 17 10.
Pubmed: Author and Title
Google Scholar: Author Only Title Only Author and Title

Rovenich, H., Boshoven, J.C. and Thomma, B.P.H.J. (2014) Filamentous pathogen effector functions: Of pathogens, hosts and microbiomes. Curr. Opin. Plant Biol. 20, 96–103.
Pubmed: Author and Title
Google Scholar: Author Only Title Only Author and Title

Rovenich, H., Zuccaro, A. and Thomma, B.P. (2016) Convergent evolution of filamentous microbes towards evasion of glycan-triggered immunity. New Phytol. 212, 896–901.
Pubmed: Author and Title
Google Scholar: Author Only Title Only Author and Title

Roy, A., Kucukural, A. and Zhang, Y. (2010) I-TASSER: a unified platform for automated protein structure and function prediction. Nat Protoc 5, 725–738.
Pubmed: Author and Title
Google Scholar: Author Only Title Only Author and Title

Sanchez-Vallet, A., Mesters, J.R. and Thomma, B.P.H.J. (2015) The battle for chitin recognition in plant-microbe interactions. FEMS Microbiol. Rev. 39, 171–183.
Pubmed: Author and Title
Google Scholar: Author Only Title Only Author and Title

Sanchez-Vallet, A., Saleem-Batcha, R., Kombrink, A., Hansen, G., Valkenburg, D.J., Thomma, B.P.H.J. and Mesters, J.R. (2013) Fungal effector Ecp6 outcompetes host immune receptor for chitin binding through intrachain LysM dimerization. Elife 2, e00790.
Pubmed: Author and Title
Google Scholar: Author Only Title Only Author and Title

Sánchez-Vallet, A., Tian, H., Rodriguez-Moreno, L., et al. (2019) A secreted LysM effector protects fungal hyphae through chitin-dependent homodimer polymerization. bioRxiv, 787820.
Pubmed: Author and Title
Google Scholar: Author Only Title Only Author and Title

Schrodinger LLC (2015) The JyMOL Molecular Graphics Development Component, Version 1.8,.

Skarina, T., Xu, X., Evdokimova, E. and Savchenko, A. (2014) High-throughput crystallization screening. Methods Mol Biol 1140, 159–168.
Pubmed: Author and Title
Google Scholar: Author Only Title Only Author and Title

Takahara, H., Hacquard, S., Kombrink, A., et al. (2016) Colletotrichum higginsianum extracellular LysM proteins play dual roles in appressorial function and suppression of chitin-triggered plant immunity. New Phytol. 211, 1323–1337.
Pubmed: Author and Title
Google Scholar: Author Only Title Only Author and Title

Tang, J., Sun, Y., Han, Z. and Shi, W. (2019) An illustration of optimal selected glycosidase for N-glycoproteins deglycosylation and crystallization. Int J Biol Macromol 122, 265–271.
Pubmed: Author and Title
Google Scholar: Author Only Title Only Author and Title

Wlodawer, A., Dauter, Z. and Jaskolski, M. (2017) Protein crystallography: methods and protocols. Humana Press 1607, 672.
Pubmed: Author and Title
Google Scholar: Author Only Title Only Author and Title

Xu, C. and Ng, D.T. (2015) Glycosylation-directed quality control of protein folding. Nat. Rev. Mol. Cell Biol. 16, 742–752.
Pubmed: Author and Title

Google Scholar: Author Only Title Only Author and Title

Yang, J. and Zhang, Y. (2015) I-TASSER server: new development for protein structure and function predictions. Nucleic Acids Res. 43, W174-81.

Pubmed: Author and Title
Google Scholar: Author Only Title Only Author and Title

Zeng, T., Rodriguez-Moreno, L., Mansurkhodzaev, A., et al. (2020) A lysin motif effector subverts chitin-triggered immunity to facilitate arbuscular mycorrhizal symbiosis. New Phytol. 225, 448–460.

Pubmed: Author and Title
Google Scholar: Author Only Title Only Author and Title

Zhang, X.-C., Wu, X., Findley, S., Wan, J., Libault, M., Nguyen, H.T., Cannon, S.B. and Stacey, G. (2007) Molecular Evolution of Lysin Motif-Type Receptor-Like Kinases in Plants. Plant Physiol. 144, 623–636.

Pubmed: Author and Title
Google Scholar: Author Only Title Only Author and Title

Zipfel, C. (2008) Pattern-recognition receptors in plant innate immunity. Curr. Opin. Immunol. 20, 10–16.

Pubmed: Author and Title
Google Scholar: Author Only Title Only Author and Title

SUPPORTING INFORMATION LEGENDS